Available online at www.sciencedirect.com
ScienceDirect
Earth and Planetary Science Letters 251 (2006) 241–253
EPSL
www.elsevier.com/locate/epsl

Thermal diffusivity of felsic to mafic granulites at elevated temperatures

Labani Ray [a,b,*], H.-J. Förster [c], F.R. Schilling [b], A. Förster [b]

[a] National Geophysical Research Institute, Uppal Road, Hyderabad 500 007, India
[b] GeoForschungsZentrum Potsdam, Telegrafenberg, 14473 Potsdam, Germany
[c] Institute of Earth Sciences, University of Potsdam, P.O. Box 601553, 14415 Potsdam, Germany

Received 15 December 2005; received in revised form 1 September 2006; accepted 6 September 2006
Available online 20 October 2006
Editor: C.P. Jaupart

Abstract

The thermal diffusivity of felsic and intermediate granulites (charnockites, enderbites), mafic granulites, and amphibolite-facies gneisses has been measured up to temperatures of 550 °C using a transient technique. The rock samples are from the Archean and Pan-African terranes of the Southern Indian Granulite Province. Thermal diffusivity at room temperature (D_{RT}) for different rock types ranges between 1.2 and 2.2 mm^2 s^{-1}. For most of the rocks, the effect of radiative heat transfer is observed at temperatures above 450 °C. However, for few enderbites and mafic granulites, radiative heat transfer is negligible up to 550 °C. In the temperature range of conductive heat transfer, i.e., between 20 ° and 450 °C, thermal diffusivity decreases between 35% and 45% with increasing temperature. The temperature dependence of the thermal diffusivity is directly correlated with the thermal diffusivity at room temperature, i.e., the higher the thermal diffusivity at room temperature, D_{RT}, the greater is its temperature dependence. In this temperature range i.e., between 20 and 450 °C, thermal diffusivity can be expressed as $D = 0.7\ \text{mm}^2\ \text{s}^{-1} + 144\ \text{K}\ (D_{RT} - 0.7\ \text{mm}^2\ \text{s}^{-1})/(T - 150\ \text{K})$, where T is the absolute temperature in Kelvin. At higher temperatures, an additional radiative contribution is observed according to CT^3, where C varies from 10^{-9} to 10^{-10} depending on intrinsic rock properties (opacity, absorption behavior, grain size, grain boundary, etc). An equation is presented that describes the temperature and pressure dependence thermal diffusivity of rocks based only on the room-temperature thermal diffusivity. Room-temperature thermal diffusivity and its temperature dependence are mainly dependent on the major mineralogy of the rock. Because granulites are important components of the middle and lower continental crust, the results of this study provide important constraints in quantifying more accurately the thermal state of the deeper continental crust.

Keywords: thermal diffusivity; thermal conductivity; temperature dependence; granulites; India

1. Introduction

Granulitic rocks are considered to be major component of the middle and lower continental crust [1]. Therefore, precise knowledge of their thermal transport properties (thermal diffusivity and thermal conductivity) at elevated

* Corresponding author. National Geophysical Research Institute, Uppal Road, Hyderabad 500 007, India. Tel.: +91 40 23434700; fax: +91 40 27171564/23434651.
E-mail addresses: labani_ngri@rediffmail.com (L. Ray), forhj@gfz-potsdam.de (H.-J. Förster), fsch@gfz-potsdam.de (F.R. Schilling), for@gfz-potsdam.de (A. Förster).

0012-821X/$ - see front matter © 2006 Elsevier B.V. All rights reserved.
doi:10.1016/j.epsl.2006.09.010

temperatures and pressures is vital for correctly inferring the thermal state of the continental lithosphere.

In the last few decades, numerous studies on temperature and pressure dependence of the thermal transport properties have been carried out for igneous, metamorphic, and sedimentary upper crustal rocks (e.g., [2–13]). Adequate studies of granulitic rocks are rare [10,14]. The thermal properties of felsic, intermediate, and mafic granulites are poorly known. Specifically for the mafic lower crust, the thermal transport properties of rocks compositionally equivalent to mafic granulites (e.g., gabbros, basalts, amphibolites) often were used in thermal modeling [15] to compensate the lack of data. Because these igneous and amphibolite-facies metamorphic rocks are chemically, but usually not mineralogically close to mafic granulites, this procedure is a poor alternative and must be viewed with caution.

In the present study, the thermal diffusivity of felsic and intermediate granulites (charnockites, enderbites), mafic granulites, and amphibolite-facies gneisses (ortho- and mafic paragneisses) has been measured at ambient condition and at elevated temperatures up to 550 °C. This range in temperature is consistent with that usually determined in the crustal portion of thermally stable continental terranes [15]. The sample material, which experienced different P–T conditions of metamorphism, represents rocks from the Achean and Pan-African Terranes of the Southern Indian Granulite Province, one of the largest granulite terranes on earth. The aim of this study is two-fold: First, it expands the poor database on the temperature dependence of the thermal diffusivity of middle and lower crustal rocks. Second, it provides a simplified equation, which can be used to calculate thermal diffusivity of granulites at elevated temperature from their thermal diffusivity at room temperature.

2. Geological background

In the southern Indian shield, a ~30-km-thick crustal pile is exposed at the surface (Fig. 1). From the north to the

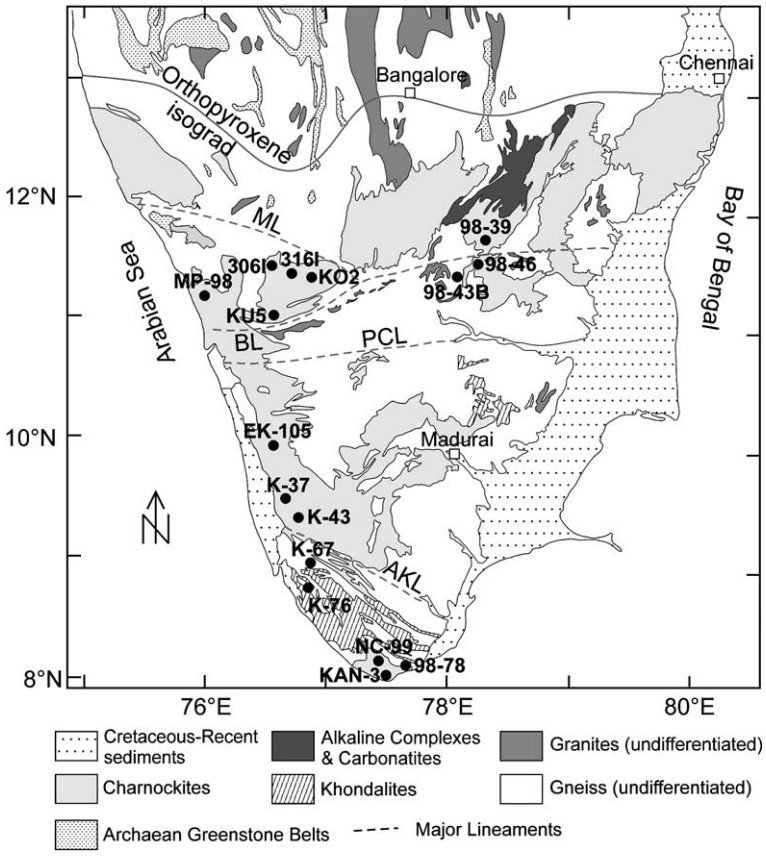

Fig. 1. Geological map of the Southern Indian Granulite Province (modified after the Geological Survey of India, 1998). The Major lineaments are: Moyar (ML), Bhavani (BL), Palghat Cauvery (PCL), and Achankovil (AKL). The Northern Block, between orthopyroxene isograd and the PCL, predominantly consists of Late-Archean granulites. The Southern Block, south of the PCL, is mainly formed by Pan-African granulites. The AKL divides the Southern Block into the Madurai Block and the Kerela Khondalite Belt. Sample locations are shown by solid circles.

south, its metamorphic grade gradually changes from greenschist facies (300 MPa) through amphibolite facies to granulite facies (1.1 GPa) [16,17]. The area between the orthopyroxene isograd and the Palghat Cauvery Lineament is known as the Northern Block (NB), where granulites are exposed providing the opportunity to study directly the middle to lower continental crust. The rocks of the Northern Block have protoliths ages between ~3.3 Ga and 2.5 Ga and were metamorphosed during the late Archean (~2.5 Ga) [18–22]. These granulites formed at pressures between 700 MPa and 1.1 GPa and temperatures ranging from 700 to 850 °C [22–26]. However, rocks of younger protoliths (~2 Ga) occur in the western part of NB (south of Nilgiri hills), which were metamorphosed during Pan-African time [27–29]. The granulitization gave rise to transformation of granites, tonalite–trondjhemite–granodiorite (TTG) gneisses, and mafic igneous rocks to charnockites, enderbites, and mafic (two-pyroxene) granulites, respectively. These rocks experienced their maximum *P–T* imprint near the Palghat Cauvery Lineament (PCL). Granulites of different metamorphic history occur in the Southern Block (SB), south of the PCL. The SB is subdivided into the Madurai block (MB) and the Kerala Khondalite Belt (KKB), with the Achankovil lineament (AKL) serving as the dividing line between the two. In contrast to the NB, the rocks of the Southern Block have protolith ages between ~3 Ga and 2 Ga and underwent granulite-facies metamorphism at ~550 Ma, during the Pan-African orogeny [30–32]. Metamorphic pressures of the SB are generally lower than in the NB, ranging from 500 to 700 MPa. However, evidence exists for a local, high-to ultra-high temperature metamorphism (900–1100 °C). The metamorphic *P–T–t* path shows an initial isobaric cooling followed by isothermal decompression [33–36]. The Southern Block consists of large massifs of charnockites/enderbites, khondalites, leptynites, and gneisses. Both, the NB and SB were invaded by Proterozoic anorthosites, syenites, carbonatites, and Neo-Proterozoic alkali granites [27,37–39]. The two blocks form the Southern Indian Granulite Province (SGP), which is one of the largest Precambrian granulite provinces on earth. The major geological units comprising the SGP are shown in Fig. 1, together with the location of the sixteen samples studied in the present paper.

3. Analytical methods

3.1. Thermal diffusivity

The thermal diffusivity (D) has been measured on sixteen samples from room temperature to 550 °C, i.e., the temperature range generally prevailing in the earth's crust. Measurements were done at intervals of 25 K up to 100 °C, and 50 K at temperatures above 100 °C. Rock samples have been cut in cubes of ~1 cm^3. The surfaces are prepared plane-parallel and smooth. Two cubes have been prepared from each sample. Thin silver coating (some tenth of a mm thickness) has been painted on the surface of the sample to reduce direct radiative heat transfer.

Measurements of thermal diffusivity on rock samples were carried out using a transient technique [40,41]. This technique permits measuring D in different directions up to temperatures of 1000 °C. In the furnace, a filament is placed above the front surface of the sample and produces a heat signal. One thermocouple is placed between filament and sample, without contact to either one. The second thermocouple is placed on the other side of the sample, i.e. below the sample. The heat generated from the filament increases the temperature of the upper thermocouple and simultaneously the front surface of the sample. For a small temperature interval dT, the temperature increase is approximately proportional to the heat transfer, dq. The value of dq depends on the generated heat and the absorption behavior of the upper thermocouple. This temperature signal starts a temperature equilibration process in the sample, which is monitored with the second thermocouple below the sample.

To produce a homogeneous temperature distribution within the furnace, a stainless steel tube with a high heat capacity and thermal conductivity encloses the experimental set up, to equalize temperature heterogeneities from the furnace and short-term temperature fluctuation from the furnace control. The tube is on a defined potential to effectively suppress electromagnetic induction. A furnace with bifilar winding was used to prevent electromagnetic induction and allows measuring diffusivity at high temperature. A metallic block with a high heat capacity and thermal conductivity surrounds the sample to further minimize temperature in homogeneities induced from the furnace.

The evaluation process does not need absolute temperature or transferred heat values. The transferred heat is an irregular function of time and, hence, there is no simple mathematical solution for the temperature response at the rear surface of the sample. The temperature–time ($T–t$) curve, measured with the upper thermocouple, is used to calculate a synthetic $T–t$ curve for the rear surface, taken into account ballistic radiative heat transfer and heat loss from the sample surfaces. The calculations are performed by a finite-difference method using different input values of thermal diffusivity. The temperature variation in one

element dT for a finite time interval dt between two elements is calculated using

$$dT = D\left(\frac{\Delta T}{\Delta x^2}\right)\mathrm{d}t \quad (1)$$

where Δx is the distance and ΔT is the temperature difference between the two elements. Thermal diffusivity values were varied systematically to obtain a best approximation for measured and calculated curves by a least-square algorithm.

For each temperature, five repetitive measurements were made. The average deviation in the measurement at each temperature is ≤2%, which is well within the uncertainty of the method of ≤3% [40].

3.2. Crack density

Presence of micro-cracks in rocks lower the laboratory-measured thermal diffusivity [42] and the elastic-modulus [43], therefore correction for crack density is essential for both the parameters. In addition to crack density, crack geometry and crack distribution are important parameters that influence thermal diffusivity [42]. The only independent information on crack density is available from elastically determined crack density [44] and porosity determination of the studied rocks. Therefore, in this study, crack density is estimated by measuring P- and S-wave velocity in the laboratory at dry and saturated condition, and using the O'Connell and Budiansky's model [44] (see Appendix A).

Seismic-wave velocity measurements were performed at room temperature and atmospheric pressure using the ultrasonic pulse-transmission technique [45]. An electric pulse is applied to different piezoelectric transducers of 1 MHz natural frequency to produce ultrasonic compressional and shear waves. The electric pulse is converted into elastic waves and the waves are transmitted through the rock sample. They are received and converted into electrical signals by the piezoelectric transducer placed on the other side of the sample. Because the travel time (t_P or t_S) includes transmission time of the signal through the filters and the time to convert electrical–mechanical signals, calibration was carried out with an aluminum sheet of different thickness, to derive the time constant of the ultrasonic assembly (t_{0P} or t_{0S}). Resultant travel time ($t_P - t_{0P}$ or $t_S - t_{0S}$) and sample dimension was used for calculating V_p or V_s, respectively. Velocity was measured on dry and saturated samples. For saturation, initially, the samples were heated in an oven at 60 °C, secondly, placed in an evacuated chamber and finally, saturated in water for 2–3 days. Errors in measurement of velocity resulting from inaccuracies in measurement of sample dimensions, travel time, and heterogeneities in rock texture are ≤2% (2σ).

3.3. Modal composition and major-element geochemistry

Many previous studies on thermal properties of rocks suffer from an inadequate mineralogical and geochemical characterization of the samples. As a result it is difficult to compare values for individual rock types. The mineralogical composition of our suite of samples was determined by careful examination of thin sections by point counting (1000–2000 counts). The major elements were determined by X-ray fluorescence (XRF) spectrometry using fused lithium tetraborate discs. The analyses were made using an automated Siemens SRS303AS spectrometer using an Rh tube operated at 50 kV and 45 nA.

4. Results

4.1. Sample characterization

4.1.1. Modal mineralogy

The modal composition of the studied rocks is listed in the Table 1. The massive to weakly foliated charnockites

Table 1
Modal composition (%)

	Charnockite					Enderbite				Mafic granulite				Gneiss		
														Orthogneiss	Paragneiss	
	KAN-3	NC-99	EK-105	K-37	K-43	KU-5	MP-98	98-46	98-78	98-39	316I	306I	KO2	98-43B	K-67	K-76
Quartz	32.2	34.5	26.9	19.9	0.5	44.2	36.0	25.8	21.6	7.4	2.0	3.0	1.4	16.7	30.4	24.7
Plagioclase	17.6	18.8	11.2	14.5	25.1	33.1	34.0	35.7	36.6	37.0	27.5	33.6	22.0	29.9	25.7	3.4
K-feldspar	42.7	32.0	50.7	47.6	57.0	9.2	5.0	7.3	12.6	2.0	9.6	5.9	1.4	20.6	28.8	58.3
Pyroxene	1.0	11.7	7.2	7.5	15.5	4.5	6.6	18.2	22.8	36.0	4.2	54.0	21.0	0.9	0.0	0.0
Garnet	0.0	0.0	0.0	2.4	0.0	8.4	9.0	7.0	0.2	12.0	9.0	0.0	29.2	0.0	7.0	11.0
Amphibole	0.0	0.0	1.2	0.0	0.0	0.0	0.0	0.0	0.4	0.0	46.5	0.4	0.0	27.0	0.0	0.0
Biotite	5.5	0.0	0.0	1.4	0.4	0.0	13.4	4.0	3.4	1.0	0.0	0.4	24.0	5.9	7.2	8.6
Others	1.0	3.0	2.3	6.7	1.5	0.6	6.0	2.0	2.4	4.6	1.2	3.0	1.0	4.9	0.9	4.0

Table 2
Major-element composition (wt.%)

	Charnockite					Enderbite				Mafic granulite				Gneiss		
														Orthogneiss	Paragneiss	
	KAN-3	NC-99	EK-105	K-37	K-43	KU-5	MP-98	98-46	98-78	98-39	3161	3061	KO2	98-43B	K-67	K-76
SiO_2	72.43	69.50	67.89	63.83	59.42	70.66	69.85	65.20	63.09	57.78	55.83	50.82	46.97	55.73	68.82	63.94
TiO_2	0.31	0.45	0.59	0.72	0.95	0.42	0.48	0.63	0.80	1.15	0.59	0.75	0.80	0.67	0.44	0.69
Al_2O_3	14.37	14.75	14.49	15.24	18.80	12.74	13.85	14.84	16.52	15.82	13.24	14.69	16.31	20.24	16.92	16.01
Fe_2O_3	2.38	3.61	4.37	6.12	4.02	5.77	5.08	5.65	5.92	11.23	11.18	11.54	12.71	5.03	2.49	4.98
MnO	0.02	0.04	0.06	0.10	0.08	0.10	0.06	0.06	0.06	0.16	0.20	0.18	0.19	0.06	0.01	0.06
MgO	0.73	0.70	0.58	0.45	1.30	2.24	2.24	2.37	1.90	5.27	6.36	6.32	8.09	2.76	0.94	1.20
CaO	2.65	2.83	2.60	2.53	3.09	3.76	2.84	4.33	4.44	3.45	9.56	11.22	11.40	7.07	3.12	1.87
Na_2O	3.53	3.98	3.57	3.16	3.51	2.66	3.22	3.87	3.90	3.82	1.82	3.14	1.94	5.61	4.73	1.93
K_2O	2.90	2.76	4.43	5.96	6.67	0.37	1.37	0.95	1.98	1.02	0.21	0.51	0.51	1.14	1.66	7.49
P_2O_5	0.05	0.14	0.19	0.16	0.26	0.12	0.10	0.21	0.28	0.02	0.07	0.07	0.06	0.22	0.07	0.55

are grey-green to greenish black and usually fine-to medium-grained, equigranular to slightly porphyritic. They are rich in feldspar (∑ K-feldspar+plagioclase= 51–82%; K-feldspar>plagioclase) and contain variable percentages of quartz (0.5–35) and pyroxene (1–16). Garnet, amphibole, and biotite are subordinate. The enderbites show principally the same appearance and color as the charnockites. They are poorer in feldspar (∑ K-feldspar+plagioclase=39–49%; Plagioclase>K-feldspar) relative to the charnockites. The modal abundances of quartz (22–44%), pyroxene (5–23%), garnet (0.2–9%), and biotite (0–13%) scatter over a relatively wide range. The fine-grained, equigranular, dark mafic granulites are poor in quartz (<7.4%) and contain between 23% and 40% feldspar (plagioclase » K-feldspar), but otherwise are mineralogically strongly variable. They comprise samples particularly rich in pyroxene (up to 54%), garnet (up to 29%), retrograde amphibole (up to 46%), and biotite (up to 24%), together with such almost devoid of these four species. The mafic orthogneiss is coarse-grained, containing up to cm-sized grains of light green feldspar and metallic black amphibole. Pyroxene and biotite are minor constituents. The light paragneisses are dominated by feldspars ((∑ K-feldspar+ plagioclase=62–64%) and quartz (25–30%). Biotite is permanently present (7–9%), whereas pyroxene and amphibole are missing. The rocks are coarse-grained and heterogranular. Light red garnet and white-greenish feldspars may approach sizes exceeding 1 cm.

All samples were carefully examined for anisotropy by ultrasonic and diffusivity experiments. Most of the granulite samples are massive. A minority of samples show a weak anisotropy A ($A_v=2\ (v_{max}-v_{min})/(v_{max}+v_{min})$; $A_D=2\ (D_{max}-D_{min})/(D_{max}+D_{min})$), which varies between experimental uncertainty.

4.1.2. Geochemistry

As they do mineralogically, the high-grade metamorphic rocks cover a wide range in bulk-rock composition. Their major-element compositions are compiled in the Table 2. The charnockites cover the range 59.4–72.4 wt.% SiO_2. Adopting the classification of plutonic rocks of Middlemost [46], the rocks are granodioritic (samples KAN-3, NC-99), granitic (EK105), quartz syenitic (K-37), and syenitic (K-43) in composition. The enderbites display a more restricted range in silica (63.1–70.7 wt.%) and resemble granodiorites (98–78) and tonalites. Mafic granulites have between 47.0 and 57.8 wt.% SiO_2 and are quartz dioritic to dioritic in composition. The amphibolite equals a quartz monzodiorite.

4.1.3. Crack density

The results of P and S-wave velocity measurements at dry and saturated conditions are summarized in the Table A1 (see Appendix A). The granulites show a similar velocity at dry and saturated condition, whereas the gneisses have a significantly higher velocity at saturated condition, suggesting different crack densities between the granulites and the other rocks. Indeed, the crack density in the granulites (0.001 to 0.06) is systematically lower than that in the gneisses (0.09 to 0.28). Heat transport is significantly hindered by gas filled pores, whereas penny shaped pores have a higher influence on heat transport than spherical ones [42]. The same holds true for seismic energy transported through a cracked medium [44]. Furthermore, if the pores are filled with fluids, both, sound velocity and heat can be transported without a minor reduction with respect to the non-cracked sample [42,44]. In addition, the pressure dependence of sound velocity and heat transport show a similar behavior [10]. Therefore, as a first approximation, the intrinsic

Table 3
Crack Density (ε), Correction Factor for Cracks (CFC), Density (ρ), Thermal Conductivity (λ), Thermal Diffusivity at room temperature (D_{RT}), Corrected Thermal Diffusivity (D_{COR}) and Temperature dependence thermal diffusivity ($T0A$, B, C)

	Charnockite					Enderbite				Mafic granulite				Gneiss		
														Orthogneiss	Paragneiss	
	KAN-3	NC-99	EK-105	K-37	K-43	KU-5	MP-98	98-46	98-78	98-39	316I	306I	KO2	98-43B	K-67	K-76
ε	0.002	0.059	0.010	0.024	0.053	0.033	0.028	0.018	0.011	0.001	0.072	0.025	0.038	0.287	0.090	0.147
CFC	1.001	1.054	1.025	1.023	1.041	1.015	1.061	1.017	1.015	1.009	1.063	1.026	1.028	1.367	1.106	1.211
ρ^1	2.67	2.65	2.71	2.69	2.67	2.80	2.70	2.75	2.76	2.97	3.04	3.23	3.24	2.84	2.74	2.76
λ^1	2.81	2.76	2.62	2.50	2.33	3.50	3.22	2.75	2.53	2.47	2.56	2.27	2.60	2.20	2.94	2.43
D_{RT}	1.80	1.72	2.10	1.66	1.25	2.16	2.13	1.51	1.50	1.17	1.28	1.21	1.29	1.15	1.77	1.73
D_{COR}	1.81	1.82	2.13	1.68	1.31	2.22	2.18	1.53	1.53	1.20	1.36	1.24	1.34	1.57	1.96	2.10
$T0$	150	150	150	150	150	150	150	150	150	150	150	150	150	150	150	150
A	0.7	0.7	0.7	0.7	0.4	0.7	0.7	0.7	0.7	0.7	0.7	0.7	0.7	0.7	0.7	0.7
B	160	166	210	140	85	220	220	148	120	70	105	78	87	125	180	203
$C\times E-10$	7.0	6.6	7.0	3.0	7.0	3.5	3.0	1.5	5.0	0.02	2.5	3.7	3.9	10.0	8.0	11.0

[1] [54].

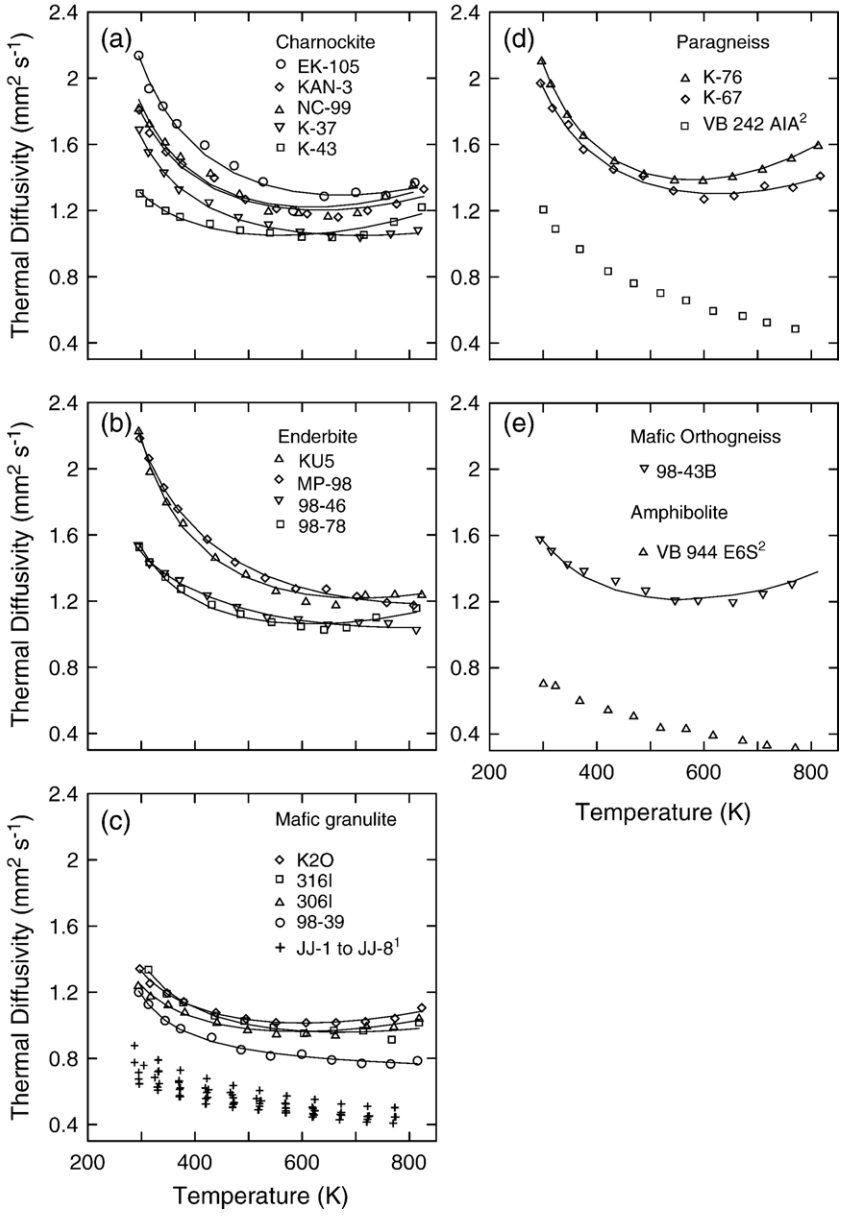

Fig. 2. Temperature dependence of thermal diffusivity of (a) charnockites, (b), enderbites, (c) mafic granulites, (d) mafic orthogneiss, and (e) paragneisses from the Southern Indian Granulite Province. Symbols reflect the average thermal diffusivity for each temperature. The solid line represents the least-square regression line for each sample. Data for mafic granulites from the Precambrian Svecoscandian Shield of Finland and Variscan metamorphic rocks (amphibolite and paragneiss) encountered by the German deep KTB borehole are shown for comparison. 1: [14], 2: [12].

diffusivity of the rock D_{rock} (without cracks) can be modeled from the observed diffusivity D_{measured} and the determined sound velocities (for details see Appendix A) according to

$$D_{\text{rock}} = D_{\text{measured}} \left(\frac{V_{\text{p}}^{\text{int}}}{V_{\text{p}}} + \frac{V_{\text{s}}^{\text{int}}}{V_{\text{s}}} \right) / 2 \qquad (2)$$

The resultant correction of thermal diffusivity for cracks is 0.5% to 8% for granulites and 10% to 35% for the gneisses (Table 3).

4.2. Thermal diffusivity

At room temperature, the thermal diffusivity of charnockites and enderbites ranges from 1.3 to 2.2 $\text{mm}^2\ \text{s}^{-1}$,

whereas that of the mafic granulites is usually lower and in the interval between 1.2 and 1.4 mm^2 s^{-1} (Table 3). The mafic orthogneiss (amphibolite) has a relatively low thermal diffusivity of 1.6 mm^2 s^{-1}, in contrast to that of the more Si-rich paragneisses (2.0–2.1 mm^2 s^{-1}). The effect of radiative heat transfer becomes visible for most of the rocks around 450 °C. However, for some enderbites and mafic granulites it is insignificant up to 550 °C. Fig. 2 is a compilation of the crack-corrected thermal-diffusivity patterns obtained in this study for metamorphic rocks from India. Thermal diffusivity data for mafic granulites, mafic orthogneisses, and paragneisses taken from the literature are plotted for comparison.

5. Discussion

5.1. Thermal diffusivity as function of modal mineralogy

The range in room-temperature thermal diffusivity (and consequently, also thermal conductivity) can be readily explained in terms of variation of modal mineralogy. Thermal diffusivity is primarily determined by the amount of quartz (Fig. 3a), which has the highest thermal diffusivity among the major minerals of the investigated rocks (average D_{quartz}=4.7 mm^2 s^{-1}, [41]). Of second-order importance is the abundance of pyroxene, amphibole, and garnet, which display intermediate diffusivities (most of them fall in a range between 1 and 2 mm^2 s^{-1}) [2,47–50]. Feldspars are of minor importance owing to their low diffusivity of usually <1 mm^2 s^{-1} [41,51–53]. Fig. 3b shows that the thermal diffusivity is also positively correlated with the bulk-rock SiO_2 content. However, the correlation of D and bulk-rock SiO_2 is weaker (correlation coefficient R=0.78) than the correlation of D with modal quartz (R=0.84). This discrepancy is reflection of the circumstance that the weight percentage of silica is only is a first-order approximation of the quartz content.

The importance of mineralogy on D is well documented for the group of mafic granulites. Thermal diffusivity of our Indian mafic granulites (1.2 to 1.4 mm^2 s^{-1}) is significantly higher than that of mafic granulites from Finland, ranging from 0.65 to 0.90 mm^2 s^{-1} [14] at room temperature (Fig. 2c). These granulites are poor in minerals of high thermal diffusivity (<2% quartz) and rich in minerals of low thermal diffusivity (35–70% feldspar), in addition to 20–45% of pyroxene+amphibole+garnet. Relative to them, the granulites from this study are slightly richer in quartz (1.4–7.4%), but higher in pyroxene+amphibole+garnet (50–60%) and lower in feldspar (25–40%) (cf.Table 1).

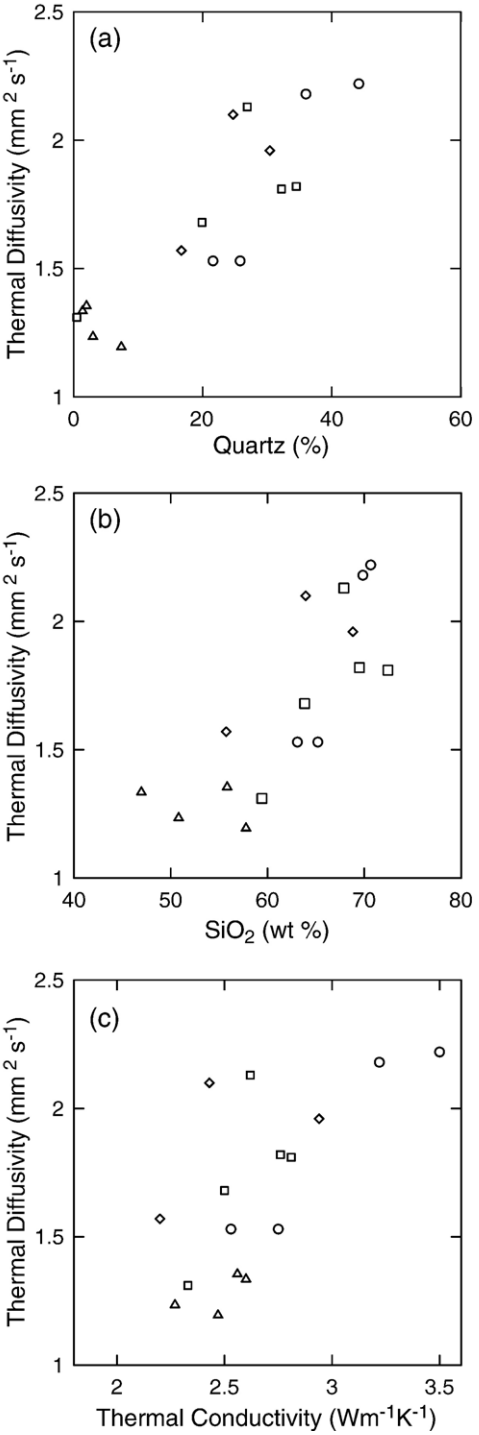

Fig. 3. Plots showing the relationships between (a) the modal content of quartz vs. thermal diffusivity, (b) the SiO_2 (wt.%) vs. thermal diffusivity, and (c) thermal conductivity vs. thermal diffusivity. Charnockites are shown by squares, enderbites by circles, mafic granulites by triangles, and the orthogneiss and the paragneisses by diamonds.

The amphibolite from the KTB borehole consists of 5% quartz, 35% feldspar, 47% amphibole, and 10% garnet and is significantly lower in room-temperature thermal diffusivity (~0.75 $mm^2\ s^{-1}$, [12]) than our mafic orthogneiss (amphibolite) containing three times more modal quartz (Fig. 2e).

Fig. 3c is a plot of thermal diffusivity versus thermal conductivity at room temperature. Thermal conductivity of our suite of samples is in the interval 2.2 to 3.4 $Wm^{-1}\ K^{-1}$ [54] and was measured using the optical scanning method [55]. Similar ranges in thermal conductivity are observed for different rock types from the study area [56,57], using the steady-state divided-bar apparatus (modified Birch-type apparatus [2], see [58]). At room temperature, thermal diffusivity matches well with the thermal conductivity ($R=0.68$) considering the measured rock density and assuming a specific heat-capacity range from 0.6 to 0.8 $Jg^{-1}\ K^{-1}$.

5.2. Thermal diffusivity as function of temperature and pressure

Among the major minerals, quartz shows the strongest and feldspar the smallest temperature dependence, and the highest versus the smallest thermal diffusivity (ca. 0.8 mm^2/s), respectively [40,41,46,51–53,59]. At temperatures below 500 °C, heat transfer in crustal rocks is mainly due to phonon conduction (lattice vibration), which is inversely proportional to temperature [60]. At higher temperature, radiative heat transfer (photons) starts playing a role, which can be treated, as a first approximation, as proportional to the cube of temperature [61]. The temperature dependence of thermal diffusivity can, therefore, be approximated by

$$D = A + \frac{B}{T - T0} + CT^3 \tag{3}$$

where A, B, C and $T0$ are constants. A is the ultra-high temperature thermal diffusivity which should be equal to the Einstein (1911) approximation, D_{min} (e.g., [59]). The minimum thermal diffusivity D_{min} is defined by the inter-atomic distance l_{min} (e.g., O–Si distance) and the mean sound velocity v using Eq. (4), when $l=l_{min}$

$$D = \frac{1}{3} v \cdot l \tag{4}$$

B is the temperature dependence of phonon conduction and C is due to the radiative heat contribution. The temperature, at which radiative heat transfer starts to become significant, varies from rock to rock and depends upon intrinsic properties such as opacity, absorption behavior, grain size, grain boundary, and others (see, [62,63]). Furthermore, the experimentally observed heat transfer strongly depends on the sample size and, therefore, on the experimental setup [64].

At temperatures above 500 °C, dehydration as well as generation of thermally induced cracks further affects the thermal transport properties. The effect of the α–β transition of quartz at 573 °C is associated with a decrease in thermal transport properties around that temperature [41]. Above that temperature, thermal diffusivity usually starts to increase due to radiative heat transfer [41,64]. In our study, radiative heat transfer became effective for most of the charnockites, enderbites, mafic granulites, and gneisses at about 450 °C. However, for some enderbites and mafic granulites, this phenomenon did not occur up to 550 °C. Kukkonen et al. [14] have not observed the radiative heat-transfer effect up to 850 °C for mafic granulites, which seems to be the result of the experimental setup used rather than reflect different modal compositions of the rocks.

By keeping A, B, C, and $T0$ variable in the Eq. (3), A and $T0$ vary between 0.70 and 0.76 and 100 and 200, respectively, for the rock studied by least square regression (Appendix A, Table A2).

It is possible to reduce the number of independent parameters in Eq. (3) without a significant loss of information. As parameter A defines the high-temperature limit of phononic heat transfer, this value is taken as 0.7 mm^2/s, i.e., the Einstein-limit of heat transfer defined by the mean sound velocity and mean free path length (see, Eq. (4)). If $T0$ is set to 150 K in Eq. (3), an optimum approximation is achieved for all samples examined. Only two independent parameters remain, describing the phononic heat transfer (B) and the radiative contribution (C) (Table 3). These relations have been considered in the formulation of a generalized equation for the estimation of thermal diffusivity at elevated temperatures (Eq. (5)). Accordingly, the thermal diffusivity (D) of granulitic rocks can be expressed as

$$D = 0.7 mm^2 s^{-1} + 144\ K \frac{D_{RT} - 0.7 mm^2 s^{-1}}{(T - 150\ K)} + CT^3 \tag{5}$$

where T is absolute temperature in Kelvin.

According to Eq. (5), the phononic part of thermal diffusivity in the temperature range 20 to 450 °C is properly described from the room temperature value of thermal diffusivity only. At higher temperatures, an additional radiative contribution has to be taken into account, which is given by CT^3. In granulites, C varies from 10^{-9} to 10^{-10} depending upon intrinsic properties of the rock (opacity, absorption behavior, grain size, grain boundary, and others), experimental setup, and sample

geometry (see, [62–64]). The four-parameter fit Eq. (3) and the two-parameter fit Eq. (5) describe the diffusivity pattern at elevated temperature similarly well within the experimental uncertainties. The simplified expression Eq. (5) is, therefore, adequate to describe the temperature dependence of D for granulitic rocks in general.

In a first approximation, according to Eq. (4), thermal diffusivity varies as a function of pressure (e.g. [65]) at the same order of magnitude (10% GPa^{-1}) as seismic velocity varies with pressure [43], taking into account that mainly the mean free path length depends on temperature. Earlier studies of high-pressure thermal diffusivity showed that the thermal diffusivity increases by 2.5% GPa^{-1} for mafic rocks [14], by 13% GPa^{-1} for granites, and by 5–10% GPa^{-1} for amphibolites and gneisses [8,12]. Thus, first-order pressure correction of 10% GPa^{-1} seems to be appropriate for the rocks under investigation and seems to describe the experiments within their experimental uncertainties.

The parameter, which has the greatest impact on the temperature dependence of the thermal diffusivity, is the room-temperature thermal diffusivity (Eq. (5)), which itself depends on the mineralogical composition of the rock. Rocks with high thermal diffusivities at room temperature display a greater proportional decrease in D with increasing T, and vice versa (e.g., Fig. 2a to 2e), well described by Eq. (5). For the granulites and gneisses from this study, the decrease in thermal diffusivity is between 35% and 45% in the temperature range between 20 and 450 °C.

In conclusion, the room-temperature thermal diffusivity D_{RT} constitutes a parameter, which permits to describe sufficiently accurate the temperature and pressure dependence (0.1 P GPa^{-1}) of D for granulites (Eq. (6)). Thermal diffusivity as a function of temperature (T) and pressure (P) can be expressed as

$$D = \left(0.7\mathrm{mm^2s^{-1}} + 144\ \mathrm{K}\frac{D_{RT}-0.7\mathrm{mm^2s^{-1}}}{(T-150\ \mathrm{K})}\right) \times \left(1+\frac{0.1}{\mathrm{GPa}}P\right) + CT^3 \quad (6)$$

With the utilization of this equation, future thermal modeling of deep crustal sections involving granulitic rocks can be performed with the room-temperature thermal diffusivity being the only parameter to measure if heat transport by radiation can be neglected.

Acknowledgements

This research work was generously supported by the GeoForschungsZentrum Potsdam (GFZ), Germany. LR is grateful to the Director of NGRI and the Director General of the CSIR, India, for granting her leave to the GFZ, during which most of the experimental and analytical work was performed. LR is indebted to R. U.M. Rao (India) for incessant encouragement and valuable suggestions. Thanks to R. Srinivasan and S. Roy (NGRI) for the useful discussions during fieldwork and collection of samples. I. Braun and M. Raith (Bonn) are thanked for providing samples from Nilgiri area. The support of K. Gratz and M. Knoll (GFZ) in the laboratory works is specifically acknowledged. P. Vijay (NGRI) and A. Reimann (Potsdam) helped with the petrographic study. We thank the editor-in-chief C.P. Jaupart and an anonymous reviewer for their constructive comments and valuable suggestions.

Appendix A

According to O'Connell and Budiansky [44], the crack density ε for elliptical cracks (with $a>b\gg c$) can be expressed by

$$\varepsilon = \left(\frac{2N}{\pi}\right)\left(\frac{A^2}{P}\right) \quad (A1)$$

A is the area of a crack (πab), P is the perimeter and N is the number of the cracks per unity volume.

In case of circular cracks $(a=b=r)$, $\varepsilon = N^* r^3$ (A2)

The modulus of elasticity for randomly orientated dry circular cracks can be given by:

$$\bar{K} = K\left(1-\frac{16}{9}\left(\frac{1-\bar{\sigma}^2}{1-2\bar{\sigma}}\right)\varepsilon\right) \quad (A3)$$

$$\bar{G} = G\left(1-\frac{32}{45}\frac{(1-\bar{\sigma})(5-\bar{\sigma})}{2-\bar{\sigma}}\varepsilon\right) \quad (A4)$$

$$\bar{\sigma} = \sigma\left(1-\frac{16}{9}\varepsilon\right) \quad (A5)$$

If the cracks are saturated with fluid then the elastic properties of the fluid phase have to be considered and the elastic modulus can be expressed as:

$$\bar{K} = K \quad (A6)$$

$$\bar{G} = G\left(1-\frac{32}{15}\left(\frac{1-\bar{\sigma}}{2-\bar{\sigma}}\right)\varepsilon\right) \quad (A7)$$

$$\bar{\sigma} = \sigma + \frac{32}{45}\frac{(1-\bar{\sigma}^2)(1-2\sigma)}{(2-\bar{\sigma})} \quad (A8)$$

where $\bar{K}$, $\bar{G}$, and $\bar{\sigma}$ are bulk modulus, shear modulus, Poisson ratio for the cracked volume. K, G and σ are the same quantities for the uncracked volume. Seismic wave velocity can be related to the elastic modulus by the following expressions:

$$\frac{\bar{V}_p}{V_p} = \sqrt{\frac{(1-\bar{\sigma})(1+\sigma)\bar{K}}{(1-\bar{\sigma})(1-\sigma)K}} \quad \text{(A9)}$$

$$\frac{\bar{V}_s}{V_s} = \sqrt{\frac{\bar{G}}{G}} \quad \text{(A10)}$$

$$\frac{\bar{V}_p/\bar{V}_s}{V_p/V_s} = \sqrt{\frac{(1-\bar{\sigma})(1+2\sigma)\bar{K}}{(1-2\bar{\sigma})(1-\sigma)K}} \quad \text{(A11)}$$

where bar quantities are for cracked volume and others are for uncracked volume of rocks. Crack density as well as intrinsic P and S-wave velocity have been estimated from the observed seismic velocities and Poisson ratios.

The obtained crack density has been applied for the thermal diffusivity on the assumption that the same crack density will influence the thermal diffusivity in a similar way as it influences the seismic velocities (V_p and V_s). Thermal diffusivity is approximated by using

$$D_{rock} = D_{measured}\left(\frac{V_p^{int}}{V_p} + \frac{V_s^{int}}{V_s}\right)/2 \quad \text{(A12)}$$

where V_p and V_s are P and S wave velocity of the rock at dry condition and V_p^{int} and V_s^{int} are the intrinsic velocities.

Table A1
P and S-wave velocity (km s^{-1}) at dry condition (V_p^{dry}, V_s^{dry}), saturated condition (V_p^{sat}, V_s^{sat})and the intrinsic velocity (V_p^{int}, V_s^{int})

	Charnockite					Enderbite				Mafic granulite				Gneiss		
														Orthogneiss	Paragneiss	
	KAN-3	NC-99	EK-105	K-37	K-43	KU-5	MP-98	98-46	98-78	98-39	3161	3061	KO_2	98-43B	K-67	K-76
V_p^{dry}	6.28	5.93	6.00	6.12	6.23	6.40	6.21	6.28	6.48	6.57	7.15	7.20	7.35	4.61	5.71	4.85
V_s^{dry}	3.65	3.58	3.45	3.51	3.56	3.90	3.68	3.62	3.67	3.73	4.15	3.80	4.00	3.02	3.52	2.94
V_p^{sat}	6.27	6.21	6.26	6.28	6.44	6.45	6.48	6.29	6.53	6.68	7.55	7.20	7.40	5.91	6.38	6.10
V_s^{sat}	3.65	3.59	3.57	3.54	3.50	3.85	3.60	3.67	3.74	3.78	4.10	3.82	3.90	3.17	3.70	3.25
V_p^{int}	6.28	6.33	6.17	6.31	6.60	6.57	6.73	6.39	6.57	6.63	7.78	7.46	7.70	6.67	6.44	6.12
V_s^{int}	3.65	3.72	3.52	3.57	3.64	3.91	3.82	3.68	3.73	3.76	4.31	3.86	4.04	3.89	3.82	3.41

Table A2
Temperature dependence of thermal diffusivity

	Charnockite					Enderbite				Mafic granulite				Gneiss		
														Orthogneiss	Paragneiss	
	KAN-3	NC-99	EK-105	K-37	K-43	KU-5	MP-98	98-46	98-78	98-39	3161	3061	KO2	98-43B	K-67	K-76
$T0$	140	150	140	160	120	170	130	100	160	200	170	150	150	110	130	150
A	0.71	0.71	0.71	0.71	0.71	0.71	0.71	0.75	0.70	0.69	0.71	0.71	0.73	0.72	0.72	0.70
B	169.2	165.7	218.2	128.2	103.0	188.5	246.6	147.7	112.6	49.2	87.3	77.8	86.9	155.7	204.0	203.0
$C\times E-10$	5.7	6.6	5.6	2.	5.7	4.3	2.1	1.5	4.8	0.02	2.5	3.7	3.9	8.0	7.0	11.2

References

[1] J.A. Percival, D.M. Fountain, M.H. Salisbury, Exposed crustal cross-sections as windows on the lower crust, in: D.M. Fountain, R. Arculus, R.W. Kay (Eds.), Continental Lower Crust, Dev. Geotectonics, vol. 23, Elsevier Sci., Amsterdam, 1992, pp. 317–362.

[2] F. Birch, H. Clark, The thermal conductivity of rocks and its dependence upon temperature and composition, Am. J. Sci. 238 (1940) 529–635.

[3] W.L. Sibbitte, J.G. Dodson, J.W. Tester, Thermal conductivity of crystalline rocks associated with energy extraction from hot dry rock geothermal systems, J. Geophys. Res. 84 (1979) 1117–1124.

[4] K. Horai, J. Susaki, The effect of pressure on the thermal conductivity of silicate rocks up to 12 kbar, Phys. Earth Planet. Inter. 55 (1989) 292–305.

[5] J.H. Sass, A.H. Lachenbruch, T. Moses, P. Morgan, Heat flow from a scientific research well at Cajon Pass, California, J. Geophys. Res. 97 (1992) 5017–5030.

[6] U. Seipold, Pressure and temperature dependence of thermal transport properties for granites, High Temp. High Press. 22 (1990) 541–548.

[7] U. Seipold, Depth dependence of thermal transport properties for typical crustal rocks, Phys. Earth Planet. Inter. 69 (1992) 299–303.

[8] U. Seipold, The variation of thermal transport properties in the Earth's crust, J. Geodyn. 2 (1995) 145–154.

[9] U. Seipold, Temperature dependence of the thermal transport properties of crystalline rocks: a general law, Tectonophysics 291 (1998) 161–171.
[10] U. Seipold, Der Wärmetransport in kristallinen Gesteinen unter den Bedingungen der kontinentalen Kruste, Scientific Technical Report, STR01/13, GFZ Potsdam, 2001.
[11] U. Seipold, Investigations of the thermal transport properties of amphibolites: I. Pressure dependence, High Temp. High Press. 3 (2002) 299–306.
[12] U. Seipold, E. Huenges, Thermal properties of gneisses and amphibolites — high pressure and high temperature investigations of KTB-rock samples, Tectonophysics 291 (1998) 173–178.
[13] H.D. Vosteen, R. Schellschmidt, Influence of temperature on thermal conductivity, thermal capacity and thermal diffusivity for different types of rock, Phys. Chem. Earth 28 (2003) 499–509.
[14] I.T. Kukkonen, J. Jokinen, U. Seipold, Temperature and pressure dependencies of thermal transport properties of rocks: implications for uncertainties in thermal lithosphere models and new laboratory measurements of high-grade rocks in the central Fennoscandian shield, Surv. Geophys. 20 (1999) 53–59.
[15] D.S. Chapman, Thermal gradients in the continental crust, in: J.B. Dawson, D.A. Carswell, J. Hall, K.H. Wedepohl (Eds.), The Nature of the Lower Continental Crust, Geol. Soc. Spec. Publ., vol. 24, 1986, pp. 63–70.
[16] C.S. Pichamuthu, Transformations of peninsular gneiss into charnockite in Mysore state, India, J. Geol. Soc. India 2 (1961) 46–49.
[17] P. Raase, M. Raith, D. Ackermand, R.K. Lal, Progressive metamorphism of mafic rocks from greenschist to granulite facies in the Dharwar Craton of south India, J. Geol. 94 (1986) 261–282.
[18] J.J. Peucat, B. Mahabaleswar, M. Jayananda, Age of younger tonalitic magmatism and granulite metamorphism in the south Indian transition zone (Krishnagiri area): Comparison with older Peninsular gneisses from Hassan–Gorur area, J. Metamorph. Geol. 11 (1993) 879–888.
[19] J.J. Peucat, P. Vidal, J. Bernard-Griffiths, K.C. Condie, Sr, Nd and Pb isotopic systematics in the Archaean low-to high-grade transition zone of southern India: syn-accretion vs. post-accretion granulites, J. Geol. 97 (1989) 537–550.
[20] N.B.W. Harris, M. Santosh, P.N. Taylor, Crustal evolution in South India: constraints from Nd isotopes, J. Geol. 102 (1994) 139–150.
[21] C. Unnikrishnan-Warrier, M. Yoshida, H. Kagami, M. Santosh, Sm–Nd and Rb–Sr mineral isochron ages of Madras charnockite, and an evolution of garnet geochronometry in granulites, Mem. Geol. Soc. India 34 (1995) 399–412.
[22] M. Raith, C. Srikantappa, D. Buhl, H. Koehler, The Nilgiri enderbites, south India: nature and age constrains on protolith formation, high-grade metamorphism and cooling history, Precambrian Res. 98 (1999) 129–150.
[23] N.B.W. Harris, R.W. Holt, S.A. Drury, Geobarometry, geothermometry and Late Archaean geotherms from granulite facies terrains of south India, J. Geol. 90 (1982) 509–527.
[24] M. Raith, P. Raase, D. Ackermand, R.K. Lal, Regional geothermobarometry in the granulite facies terrane of South India, Trans. R. Soc. Edinb. 73 (1983) 221–244.
[25] D. Rameswar Rao, B.L. Narayana, S.N. Charan, R. Natarajan, *P–T* conditions and geothermal gradients of gneiss-enderbitic rocks: Dharmapuri area, Tamil Nadu, India, J. Petrol. 32 (1991) 539–554.
[26] J.O. Eckert Jr., R.C. Newton, Paleopressures of south Indian two-pyroxene garnet granulites from thermochemically calibrated CMAS barometers, J. Metamorph. Geol. 11 (1993) 845–854.
[27] B. Meißner, P. Deters, C. Srikantappa, H. Köhler, Geochronological evolution of the Moyar, Bhavani and Palghat shear zones of southern India: implications for east Gondwana correlations, Precambrian Res. 114 (2002) 149–175.
[28] Y.J. Bhaskar Rao, A.S. Janardhan, T. Vijaykumar, B.L. Narayana, A.M. Dayal, P.N. Talor, T.R.K. Chetty, Sm–Nd model ages and Rb–Sr isotopic systematics of charnockite gneisses across the Cauvery shear zone, southern India, Mem. Geol. Soc. India 50 (2003) 297–317.
[29] J.G. Ghosh, M.J. de Wit, R.E. Zartman, Age and tectonic evolution of the ductile shear zones in the Southern Granulite Terrane of India with implication for Gondwana studies, Tectonics 23 (2004) TC3006, doi:10.1029/2002TC001/1444.
[30] M. Jayananda, A.S. Janardhan, P. Sivasubramanian, J.J. Peucat, Geochronologic and isotopic constraints on granulite formation in the Kodaikanal area, southern India, Mem. Geol. Soc. India 34 (1995) 373–390.
[31] B. Cenki, I. Braun, M. Bröcker, Evolution of the continental crust in Kerela Khondalite Belt, southernmost India: evidence from Nd isotope mapping, U–Pb and Rb–Sr geochronology, Precambrian Res. 134 (2004) 275–292.
[32] I. Braun, M. Brocker, Monazite dating of granitic gneisses and lecogranites from Kerela Khondalite Belt, Southern India, implications for the Proterozoic crustal evolution in East Gondwana, Int. J. Earth Sci. 93 (2004) 13–22.
[33] A. Mohan, B.F. Windley, Crustal trajectory of sapphirine-bearing granulites from Ganguvarpatti, South India: evidence for an isothermal decompression path, J. Metamorph. Geol. 11 (1993) 823–826.
[34] M. Brown, M. Raith, First evidence of ultrahigh-temperature decompression from the granulite province of southern India, J. Geol. Soc. Lond. 153 (1996) 819–822.
[35] M. Raith, S. Karmakar, M. Brown, Ultra-high-temperature metamorphism and multistage decompressional evolution of sapphirine granulites from the Palni Hill Ranges, southern India, J. Metamorph. Geol. 15 (1997) 379–399.
[36] M. Satish Kumar, S.L. Harley, Reaction textures in scapolite-wollastonite-grossular calc-silicate rock from the Kerala Khondalite Belt, southern India: evidence for high-temperature metamorphism and initial cooling, Lithos 44 (1998) 83–99.
[37] A. Mohan, The Madurai granulite block, in: M. Santosh, M. Yoshida (Eds.), Archaean and Proterozoic Terrains of Southern India within East Gondwana, Gondwana Research Group, vol. 3, 1996, pp. 223–243.
[38] R.A. Wiebe, A.S. Janardhan, Metamorphism of the Oddanchatram Anorthosite, Tamil Nadu, South India Memoir, Mem. Geol. Soc. India 25 (1993) 113–117.
[39] M. Santosh, S.S. Iyer, M.B.A. Vasconcellos, J. Ensweiler, Late Precambrian alkaline plutons in southwest India: geochronologic and rare earth element constraints on Pan-African magmatism, Lithos 24 (1989) 65–79.
[40] F.R. Schilling, A transient technique to measure thermal diffusivity at elevated temperatures, Eur. J. Mineral. 11 (1999) 1115–1124.
[41] M. Höfer, F.R. Schilling, Heat-transfer in quartz, orthoclase, and sanidine at elevated temperature, Phys. Chem. Miner. 29 (2002) 571–584.
[42] F.R. Schilling, The effect of fluids on thermal diffusivity of some magmatic rocks, Phys. Chem. Earth 22 (1997) 87–91.
[43] H. Kern, R. Schmidt, T. Popp, The velocity and density structure of the 4000 m crustal segment at the KTB drilling site and their relationship to lithological and microstructural

characteristics of the rocks: a experimental approach, Sci. Drill. 2 (1991) 130–145.
[44] R. O'Connell, B. Budiansky, Seismic velocities in dry and saturated cracked solids, J. Geophys. Res. 79 (1974) 5412–5426.
[45] F. Birch, The velocity of compressional waves in rocks to 10 kbar, Part 1, J. Geophys. Res. 65 (1960) 1083–1102.
[46] E.A.K. Middlemost, Magmas and Magmatic Rocks; An Introduction to Igneous Petrology, Longman Group, London, 1985. 246 pp.
[47] H. Kanamori, N. Fujii, H. Mizutani, Thermal diffusivity measurements of rock-forming minerals from 300 °K to 1100 °K, J. Geophys. Res. 73 (1968) 595–605.
[48] M. Osako, Thermal diffusivity of olivine and garnet single crystals, Bull. Natl. Sci. Mus., Tokyo, Ser. E 20 (1997) 1–7.
[49] H. Marquardt, F.R. Schilling, K. Gratz, Thermal diffusivity of garnets as a function of temperature, Ber. Dtsch. Mineral. Ges., Beih. Eur. J. Mineral. 17 (2005) No 1.
[50] K. Horai, G. Simmon, Thermal conductivity of rock-forming minerals, Earth Planet. Sci. Lett. 6 (1969) 359–368.
[51] V.A. Magnitzki, G.J. Petrunin, R.P. Jurtschak, Temperature dependence of thermal diffusivity of feldspars (in Russian), Dokl. Akad. Nauk SSR 199 (1971) 1058–1060.
[52] M.L. Linvill, J.W. Vandersande, R.O. Pohl, Thermal conductivity of feldspar, Bull. Mineral. 107 (1984) 521–527.
[53] A.E. Beck, D.M. Darbha, H.H. Schloessin, Lattice conductivities of single-crystal and polycrystalline materials at mantle pressures and temperature, Phys. Earth Planet. Inter. 17 (1978) 35–53.
[54] Labani Ray et al., Thermophysical properties of granulites (in preparation).
[55] Y.A. Popov, D.F.C. Pribnow, J.H. Sass, C.F. Williams, H. Burkhardt, Characterization of rock thermal conductivity by high-resolution optical scanning, Geothermics 28 (1999) 253–276.
[56] Labani Ray, Crustal thermal structure of the Southern Granulite Province, India, PhD thesis, Osmania University, Hyderabad, (2002), 218 pp.
[57] Labani Ray, P. Senthil Kumar, G.K. Reddy, S. Roy, G.V. Rao, R. Srinivasan, R.U.M. Rao, High mantle heat flow in a Precambrian granulite province: evidence from Southern India, J. Geophys. Res. B108 (2003) 2084, doi:10.1029/ 2001JB000688.
[58] R.U.M. Rao, R.K. Verma, G.V. Rao, V.M. Hamza, P.K. Panda, M.L. Gupta, The heat flow studies in the Godavari valley, India, Tectonophysics 10 (1970) 165–181.
[59] D.G. Cahill, S.K. Watson, R.O. Pohl, Lower limit to the thermal conductivity of disordered crystals, Phys. Rev. B46 (1992) 6131–6140.
[60] A. Euken, Über die Temperaturabhängigkeit der Wärmeleitfähigkeit fester Nichtmetalle, Ann. Phys. Leipzig 34 (1911) 186–211.
[61] C. Clauser, Opacity — the concept of radiative thermal conductivity, in: R. Haenel, L. Rybach, L. Stegena (Eds.), Handbook of Terrestrial Heat-Flow Density Determination, Kluwer, Dordrecht, 1988, pp. 143–165.
[62] T.J. Shankland, U. Nitsan, A.G. Duba, Optical absorption and radiative heat transport in olivine at high temperature, J. Geophys. Res. 84 (1979) 1603–1610.
[63] Y. Xu, T.J. Shankland, S. Linhardt, D.C. Rubie, F. Lagenhorst, K. Klasinsk, Thermal diffusivity and conductivity of olivine, wadsleyite and ringwoodite to 20 GPa and 1373 K, Phys. Earth Planet. Inter. 143–144 (2004) 321–336.
[64] B. Gibert, F.R. Schilling, K. Gratz, A. Tommasi, Thermal diffusivity of olivine single-crystals and a dunite at high temperature: Evidence for heat transfer in the upper mantle, Phys. Earth Planet. Inter. 151 (2005) 129–141.
[65] J. Arndt, T. Bartel, E. Scheuber, F.R. Schilling, Thermal and rheological properties of granodioritic rocks from the Central Andes, North Chile, Tectonophysics 271 (1997) 75–88.